Inner-shell excitation of acetylene by electron impact

S. E. Michelin,[1] O. Pessoa,[1] H. L. Oliveira,[1] E. Veiteinheimer,[1] A. M. S. Santos,[1] M. M. Fujimoto,[2] I. Iga,[3] and M.-T. Lee[3]
[1]*Departamento de Física, UFSC, 88040-900 Florianópolis, Santa Catarina, Brazil*
[2]*Departamento de Física, UFPR, 81531-990, Curitiba, Paraná, Brazil*
[3]*Departamento de Química, UFSCar, 13565-905, São Carlos, São Paulo, Brazil*
(Received 17 May 2005; published 30 August 2005)

The distorted-wave approximation (DWA) is applied to study *K*-shell excitation in C_2H_2 by electron impact. More specifically, calculated differential and integral cross sections for the $X\,^1\Sigma_g^+ \rightarrow {}^{1,3}\Pi_g(1s\sigma_g \rightarrow 1p\pi_g)$ and $X\,^1\Sigma_g^+ \rightarrow {}^{1,3}\Pi_u(1s\sigma_u \rightarrow 1p\pi_g)$ transitions in this target in the 300–800 eV incident energy range are reported. The triplet-to-singlet ratios of respective integral cross sections, namely, RI(3:1), calculated by dividing the integral cross sections for transitions leading to the triplet core-excited states by those leading to the corresponding singlet states, are also reported as a function of incident energies. In general, our calculated sums of the generalized oscillator strength for transitions leading to the $^1\Pi_g$ and $^1\Pi_u$ excited states are in good agreement with the available experimental data. On the other hand, the present calculated integral cross sections and the corresponding data for its isoelectronic species CO are significantly different. Possible physical origins for this difference are discussed.

DOI: 10.1103/PhysRevA.72.022730 PACS number(s): 34.80.Gs

I. INTRODUCTION

Investigation on electronic excitation of molecules induced by electron impact has received considerable attention by both experimentalists and theoreticians [1]. This technique is a useful tool for the study of high-lying excited states which are formed when an inner-shell electron is promoted to an unfilled valence or Rydberg orbital. One important advantage of this technique is its ability to access dipole-forbidden transitions [2–4]. Also, due to the high localization of the *K*-shell electrons, the ionization energies as well as the shapes and energies of core-level excitation bands would not show drastic changes as one moves from the gas to the solid state. Therefore, the molecular properties such as binding energy, structural parameters, etc., obtained using gas-phase spectroscopy can be useful for studies of condensed phases.

One interesting aspect is that shape resonance can also occur in electron-impact core-excitation processes of molecules. In this case, the low-energy outgoing electron can be trapped by the potential barrier of the excited target and thus leads to the formation of temporary negative ions associated with inner-shell-excited molecules. Such resonances were observed by Harrison and King [3,4] in the measured ratios of the excitation intensities for singlet and triplet ($C_{1s}\sigma \rightarrow 2p\pi$) transitions in CO. Similar structure was also observed by Blount and Dickinson [5] in the ratio of excitation intensities of the $(C_{1s})^{-1}(2p\pi_u)$, $^{1,3}\Pi_u$ states of CO_2 by electron impact at incident energies near 313 eV.

Despite the increasing experimental investigation on electron-impact core excitation of molecules, very few theoretical studies in this field were reported in the literature. Although a solid-based *ab initio* multichannel study on this matter is desirable, computationally, the coupling between the high-energy incident electron and the low-energy exit electron is very difficult to deal with. Therefore, the distorted-wave approximation (DWA) is presently the most reliable theoretical method for such studies. Although the interchannel coupling effects are not taken into account by this theoretical formulation, the shape resonance phenomenon, i.e., the temporary trap of the low-energy scattering electron by the potential barrier of the excited target, is represented in the collisional dynamics. Recently, the DWA was applied in the studies of carbon *K*-shell core-excitation processes of CO_2 [6] and CO [7] by electron impact. The comparison between the calculated results and the available experimental data is encouraging. More recently, we reported comparative studies on electron-impact carbon *K*-shell excitation of a series of outer-valence isoelectronic molecules containing only one carbon atom, namely, CO_2, CS_2, and OCS molecules [8,9]. In those studies, we found that the cross sections for excitations from the C(1*s*) orbital of these targets are in general quite similar with each other, particularly at high incident energies. This fact can probably be explained by the fact that the C(1*s*) orbital in these molecules are essentially *atomic*, and therefore very similar from one target to another. On the other hand, for targets containing two or more carbon atoms, the molecular-orbital description of the *K*-shell wave functions would require a combination of the C(1*s*) orbitals. Therefore, they are delocalized and no longer atomic. Thus, a comparative study on inner-shell excitation involving targets with only one carbon atom and those with two or more carbon atoms would be interesting.

In this work, we present one of such studies. The electron-impact excitation cross sections from the *K*-shell orbitals of acetylene (C_2H_2) is calculated and compared with those previously calculated results for CO [7]. Experimental investigation on the electron-impact *K*-shell excitation of C_2H_2 was reported by Miranda *et al.* [10] and Hitchcock *et al.* [11]. Particularly at incident energies of 1290 and 1300 eV, the experimental generalized oscillator strengths (GOSs) were reported [10,11]. Also a theoretical study based on the first Born approximation (FBA) is also reported by Miranda *et al.* [10]. However, to our knowledge, there are no reported theoretical studies for inner-shell excitation of C_2H_2 beyond the FBA.

The organization of the present article is as follows. In Sec. II, an outline of the theory used is presented, providing a few details of the calculations. In Sec. III a comparison of our calculated data with the theoretical and experimental results available in the literature is presented, where we also present a brief conclusion remark.

II. THEORY

Since the detailed basic theory has already been presented elsewhere [12–15], only a brief overview is provided here.

The differential excitation cross sections (DCSs) for electron-molecule scattering averaged over molecular orientations are given by

$$\frac{d\sigma}{d\Omega} = \frac{1}{8\pi^2}\int d\alpha \sin\beta\, d\beta\, d\gamma |f(\hat{k}_i', \hat{k}_f')|^2 \tag{1}$$

where $\hat{k}_f'(\hat{k}_i')$ is the direction of the scattered (incident) electron linear momentum in the laboratory frame (LF), whereas the direction of the incident electron linear momentum is taken as the LF z axis. (α, β, γ) are the Euler angles which define the direction of the molecular principal axis. The body-frame amplitude $f(\hat{k}_i, \hat{k}_f)$ is related to the T-matrix elements by the equation

$$f(\hat{k}_i, \hat{k}_f) = -2\pi^2 T_{if}, \tag{2}$$

and is related to the LF scattering amplitude by usual transformations.

In the DWA framework, the transition T matrix is given by

$$T_{if} = \langle \varphi_1 \Psi_{k_f}^{(-)} | U_{se} | \varphi_0 \Psi_{k_i}^{(+)} \rangle \tag{3}$$

where φ_0 and φ_1 are the initial and final target wave functions, respectively. These wave functions are Slater determinants with appropriate symmetries. $\Psi_{k_i}^{(+)}$ and $\Psi_{k_f}^{(-)}$ are the initial and final distorted continuum wave functions with the outgoing- $(+)$ and incoming-wave $(-)$ boundary conditions, respectively. U_{se} is the static-exchange potential operator. The distorted wavefunctions are solutions of the Lippmann-Schwinger equation

$$\Psi_{\vec{k}}^{(\pm)} = \Phi_{\vec{k}} + G_0^{(\pm)} U \Psi_{\vec{k}}^{(\pm)} \tag{4}$$

with $G_0^{(\pm)}$ being the free-particle Green's operator with appropriate boundary conditions, and $\Phi_{\vec{k}}$ is the plane wave function, with linear momentum $\vec{k}$. The wave functions $\Psi_{k_i}^{(+)}$ and $\Psi_{k_f}^{(-)}$ were calculated using the iteractive Schwinger variational method (ISVM) [16] in the static-exchange field of the ground- and excited-state target, respectively.

The electronic excitation T matrix can be partial-wave expanded as

$$T_{if} = (2/\pi)\sum_{lm}\sum_{l'm'} \frac{i^{l-l'}}{k_i k_f} T_{lml'm'} Y_{lm}^*(\hat{k}_i) Y_{l'm'}(\hat{k}_f) \tag{5}$$

where $T_{lml'm'}$ is the partial T-matrix element given by

$$T_{lml'm'} = \langle \varphi_1 \Psi_{k_f l'm'}^{(-)} | U_{se} | \varphi_0 \Psi_{k_i lm}^{(+)} \rangle. \tag{6}$$

Finally, the LF DCS is represented in a j_t basis [17] as:

$$\frac{d\sigma}{d\Omega}(n \leftarrow 0) = SM_n \frac{k_f}{k_i} \sum_{j_t m_t m_t'} \frac{1}{(2j_t+1)} |B_{m_t m_t'}^{j_t}(n \leftarrow 0, k_i, k_f', \hat{r}')|^2, \tag{7}$$

where $\vec{j}_t = \vec{l}' - \vec{l}$ is the transferred angular momentum during the collision, m_t' and m_t are the projections of j_t along the laboratory and molecular axis, respectively. The S factor is obtained from summing over final and averaging over initial spin sublevels, and M_n is the orbital-angular-momentum projection degeneracy factor of the final target state. In Eq. (7), $B_{m_t m_t'}^{jt}$ is the coefficient of the j_t-basis expansion of the LF scattering amplitudes and is given by

$$B_{m_t m_t'}^{j_t}(\Omega') = \sum_{l'lm'm} (-1)^m a_{ll'mm'}(ll'0m_t | j_t m_t) \times (ll'mm' | j_t m_t') Y_{lm_l}(\Omega') \tag{8}$$

where the dynamical coefficients $a_{ll'mm'}$ can be written in terms of fixed-nuclei partial-wave components of the electronic portion of the transition matrix elements as

$$a_{ll'mm'}(n \leftarrow 0, k_i) = -(1/2)\pi[4\pi(2l'+1)]^{(1/2)} i^{l'-l} \times \langle k_f lm, n | T | k_i l'm', 0 \rangle. \tag{9}$$

For the transitions leading to the triplet excited states, only the exchange part of the T matrix is needed. The cross sections are calculated via Eq. (7) where a direct summation over (lm) up to some truncation parameters (l_c, m_c) is performed. On the other hand, for the transitions leading to the singlet excited states, the partial-wave expansion of the transition T matrices was also truncated at the same parameters (l_c, m_c). Contributions from higher partial waves were taken into account via the Born-closure procedure [12]. Using this procedure, $B_{m_t m_t'}^{jt}$ is given by

$$B_{m_t m_t'}^{j_t}(\hat{k}') = B_{m_t m_t'}^{Born, j_t}(\hat{k}_f') + \sum_{l'lmm'} (-1)^m (i)^{l-l'} (2l+1)^{-1} \times (T_{ll'mm'}^S - T_{ll'mm'}^{Born})(l-m, l'm' | j_t m_t') \times (l0, l'm_t | j_t m_t) Y_{l'm_t}(\hat{k}_f') \tag{10}$$

where $B_{m_t m_t'}^{Born,jt}(\hat{k}_f')$ is the j_t-basis representation of the Born scattering amplitude, defined as

$$B_{m_t m_t'}^{Born, j_t}(\hat{k}_f') = \frac{(2j_t+1)}{8\pi^2} \frac{k_f}{i\pi^{(1/2)}} \int d\hat{R}' f^{Born}(\hat{R}'; \hat{k}_f') D_{m_t m_t'}^{j_t^*}(\hat{R}') \tag{11}$$

where $D_{m_t m_l'}^{jt^*}(\hat{R}')$ are the usual rotation matrices. The $T_{ll'mm'}^{Born}$ is the Born partial-wave T-matrix element given by:

$$T^{Born}_{ll'mm'} = \langle S_{klm}|U_{st}|S_{kl'm'}\rangle \tag{12}$$

where U_{st} is the reduced static potential and S_{klm} are the partial-wave components of the free-particle wave function.

Moreover, the integral cross sections (ICSs) are obtained by integrating the DCSs over all scattering angles according to the formula

$$\sigma = \int \frac{d\sigma}{d\Omega}(\theta,\phi)d\Omega. \tag{13}$$

The ground-state configuration of the C_2H_2 molecule is represented by a near-Hartree-Fock wave function. These wave functions are generated by a self-consistent-field (SCF) calculation using a standard $[11s6p]/[5s4p]$ contracted Gaussian basis [18] augmented by three s (α=0.0453, 0.0157, and 0.00537), two p (α=0.03237 and 0.00734), and one d (α=0.823) uncontracted functions on the carbon centers, and a standard $[5s]/[3s]$ contracted Gaussian basis [18] augmented by one s (α=0.0473), three p (α=1.1233, 0.2711, and α=0.0697), and one d (α=0.5371) uncontracted functions on the hydrogen centers. At the experimental equilibrium geometry (R_{C-H}=2.0041 a.u. and R_{C-C}=2.2738 a.u.), this basis set gives a SCF energy of −76.848 a.u. The same basis set is also used to calculate the wave function of the lowest $^{1,3}\Pi_{u,g}$ excited states using an improved virtual orbital (IVO) approximation [19]. The calculated vertical excitation energies for the $(1\sigma_g \rightarrow 1\pi_g)$ singlet and triplet transitions at the equilibrium geometry of the ground state are 297.326 and 296.502 eV, respectively, and for the $(1\sigma_u \rightarrow 1\pi_g)$ singlet and triplet transitions are 297.2501 and 296.3973 eV, respectively. These values can be compared with the Hartree-Fock frozen-core calculations in which the corresponding results for the singlet transitions are 297.37 and 297.29 eV [10] and the experimental results $(C_{1s})^{-1}\Pi$ by Harrison and King [4] of 285.81 eV. In addition, our calculated singlet-triplet energy splitting, for the $(1\sigma_g \rightarrow 1\pi_g)$ is 0.853 eV and that for the $(1\sigma_u \rightarrow 1\pi_g)$ transition is 0.824 eV, respectively, in reasonable agreement with the estimated value of 0.5 eV by Harrison and King [4].

III. RESULTS AND DISCUSSION

We are aware of theoretical and/or experimental results of DCSs for electron-impact core excitation of C_2H_2 in the literature. Nonetheless, the comparison of the calculated DCSs itself is interesting. Figures 1–3 present our calculated DW DCSs for the electron-impact $X\,^1\Sigma_g^+ \rightarrow {}^{1,3}\Pi_u$ and $X\,^1\Sigma_g^+ \rightarrow {}^{1,3}\Pi_g$ transitions in C_2H_2 at some selected incident energies. It is interesting to observe that the calculated DCSs for the transitions leading to the triplet excited states are quite similar, whereas those leading to the singlet excited states are significantly different, particularly at the lower end of incident energies. The reason for this difference is rather easy to understand since the $X\,^1\Sigma_g^+ \rightarrow {}^1\Pi_u$ is a dipole-allowed transition whereas the $X\,^1\Sigma_g^+ \rightarrow {}^1\Pi_g$ is dipole forbidden, but quadrupole allowed. On the other hand, the similarity of the DCSs for the transitions leading to the $^3\Pi_{u,g}$ excited states is somehow unexpected. For these singlet-to-triplet transitions only the electron exchange mechanism contributes to the excitation dynamics. One expects that the bonding character of the $1\sigma_g$ orbital, as compared to that of the antibonding $1\sigma_u$ orbital, may lead to some differences in the calculated DCSs for these transitions. At high incident energies, (see Fig. 3) even the calculated DCSs for the $X\,^1\Sigma_g^+ \rightarrow {}^1\Pi_g$ and $X\,^1\Sigma_g^+$

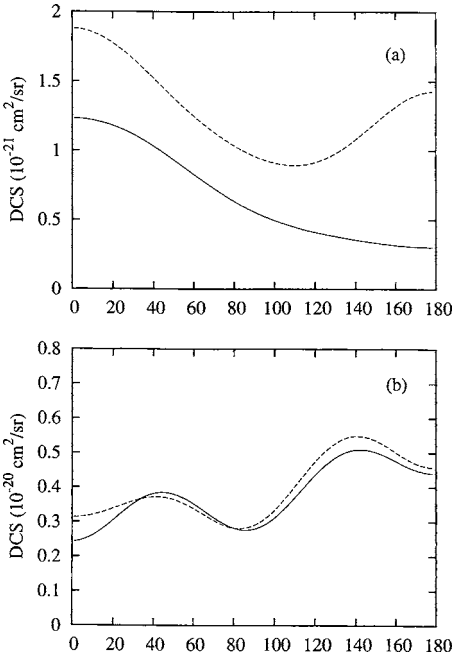

FIG. 1. Calculated DCS for (a) solid line, $1\sigma_g \rightarrow 1\pi_g$; dashed line, $1\sigma_u \rightarrow 1\pi_g$ singlet excitations; and (b) solid line, $1\sigma_g \rightarrow 1\pi_g$; dashed line, $1\sigma_u \rightarrow 1\pi_g$ triplet excitations for the e^--C_2H_2 at incident energy of 302 eV.

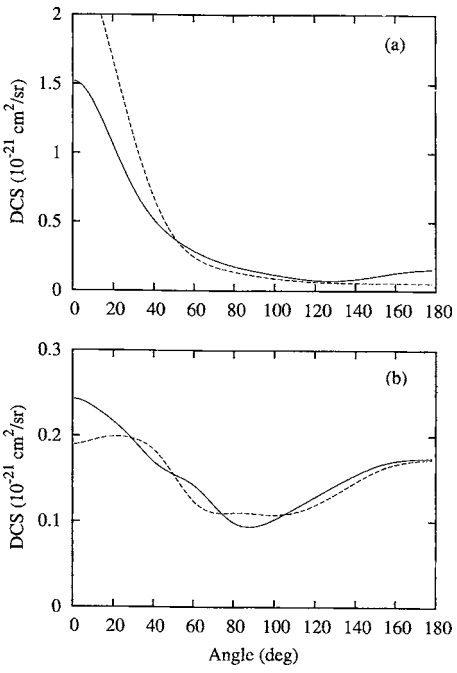

FIG. 2. Same as Fig. 1, but at incident energy of 400 eV.

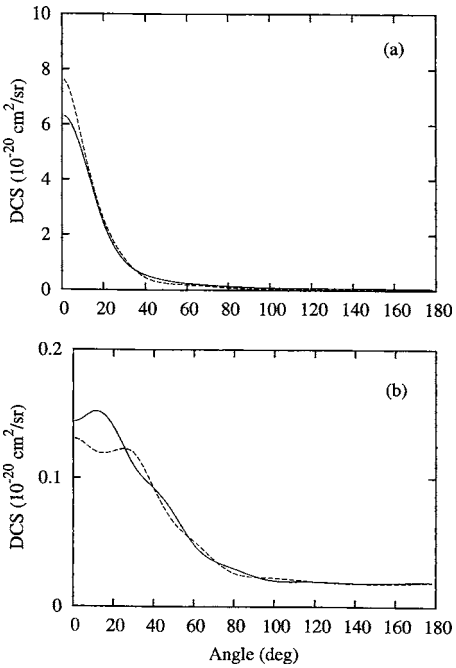

FIG. 3. Same as Fig. 1, but at incident energy of 600 eV.

$\rightarrow {}^1\Pi_u$ transitions become similar, which may indicate that the effects of the overlap of C(1*s*) orbitals of two carbon atoms become less important for fast incident electrons.

In Fig. 4 we present our GOSs calculated using both DWA and FBA for the singlet $(1\sigma_g \rightarrow 1\pi_g)$ and $(1\sigma_u \rightarrow 1\pi_g)$ transitions in C_2H_2 at 1290 eV incident energy and

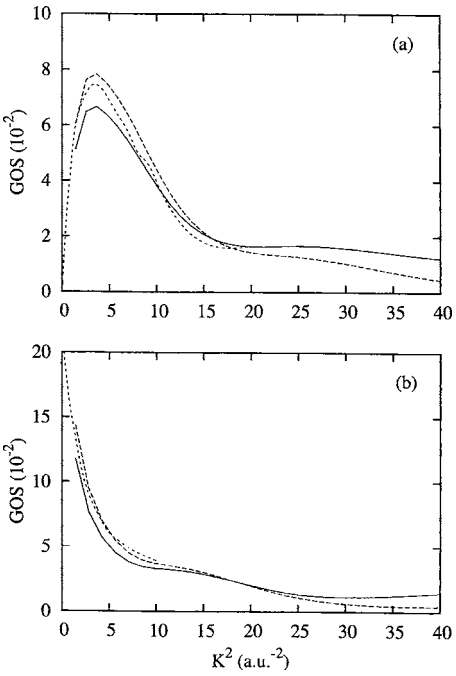

FIG. 4. Calculated GOS as a function of K^2 for electron impact: (a) $1\sigma_g \rightarrow 1\pi_g$ and (b) $1\sigma_u \rightarrow 1\pi_g$ singlet excitations for e^--C_2H_2 at 1290 eV. Solid line, present results using DWA; dashed line, present results using first Born approximation; dotted line, FBA results of Miranda *et al.* [10].

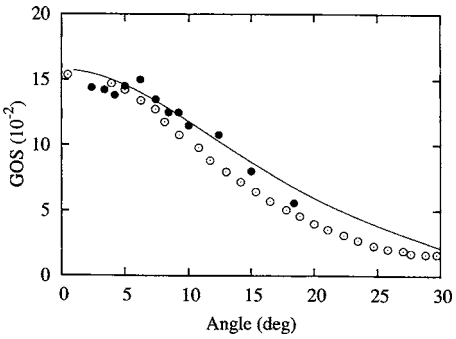

FIG. 5. Angular distribution of summed GOS for the $1\sigma_g \rightarrow 1\pi_g$ and $1\sigma_u \rightarrow 1\pi_g$ singlet transitions in C_2H_2 at incident energy of 1290 eV. Solid line, present DWA results; solid circles, experimental results from Miranda *et al.* [10]; open circles, experimental results from Hitchcock *et al.* [11], measured at 1300 eV.

compare them with the corresponding results from Miranda *et al.* [10], calculated using the FBA and the Hartree-Fock type of target wave function. The dipole-forbidden character of the $X\ {}^1\Sigma_g^+ \rightarrow {}^1\Pi_g$ transition is clearly revealed [see Fig. 4(a)] as the GOS tends to null when the magnitude of the momentum-transfer vector (K) approaches zero. Quantitatively, there is a generally good agreement between our FBA results and those of Miranda *et al.* [10]. The agreement between the DWA GOS and FBA GOS is also fairly good, particularly in the region of small K.

In Fig. 5 our DW GOSs calculated at 1290 eV for the singlet $1\sigma_{g,u} \rightarrow 1\pi_g$ transitions are compared with the experimental results of Miranda *et al.* [10] and Hitchcock *et al.* [11]. Both experiments were unable to resolve the $X\ {}^1\Sigma_g^+ \rightarrow {}^1\Pi_g$ transition from the $X\ {}^1\Sigma_g^+ \rightarrow {}^1\Pi_u$ transition. Therefore, our calculated GOSs for these two excitations are also summed up, in order to compare with the experimental data. In general, our DW GOSs are in good agreement with both experimental data, which is encouraging.

In Fig. 6, we show our calculated ICSs in the 300–800 eV energy range for the $(1\sigma_g \rightarrow 1\pi_g)$ and $(1\sigma_u \rightarrow 1\pi_g)$ singlet and triplet transitions in the C_2H_2 molecule. The calculated ICSs for the singlet and triplet $(2\sigma \rightarrow 2\pi)$ transitions in CO are also shown for comparison. The CO is chosen because this molecule has only one carbon atom, therefore its 2σ (C 1s) orbital is essentially atomic. Moreover, CO is isoelectronic with C_2H_2. As expected, the calculated ICSs for the transitions leading to the singlet excited states show an increase with increasing incident energy, meanwhile those leading to triplet excited states decrease with energy, which indicates that the electron exchange effects become less relevant at higher incident energies. Still on qualitative aspects, the calculated ICSs for both transitions leading to the ${}^3\Pi_g$ and ${}^3\Pi_u$ excited states have shown two resonances, centered at about 309 and 343 eV, respectively. Two very weak resonances are also seen in the ICS for the $X\ {}^1\Sigma_g^+ \rightarrow {}^1\Pi_g$ transition, centered at 323 and 345 eV, respectively, whereas only one weak resonance at about 311 eV is seen in the ICS for the $X\ {}^1\Sigma_g^+ \rightarrow {}^1\Pi_u$ transition in C_2H_2. On the other hand, a very strong resonance is seen in the ICS for the triplet $(2\sigma \rightarrow 2\pi)$ transition in CO at about

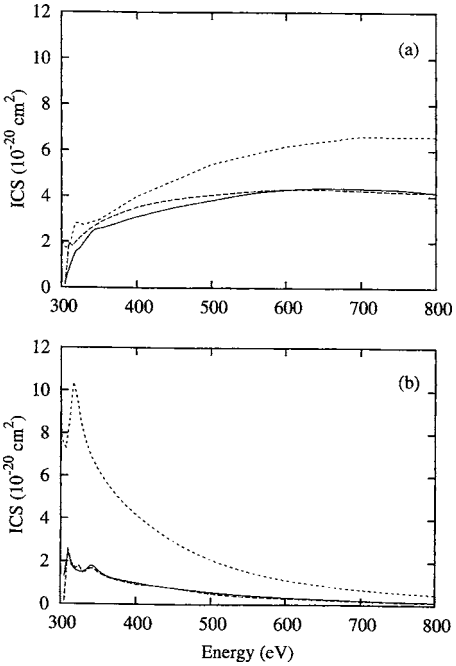

FIG. 6. Calculated DWA ICS for electron-impact (a) singlet and (b) triplet transitions in the 300–800 eV range. Solid line, $1\sigma_g \rightarrow 1\pi_g$; dashed line, $1\sigma_u \rightarrow 1\pi_g$ transitions in C_2H_2; dotted line, ICS for the singlet $2\sigma \rightarrow 2\pi$ transition in CO.

318 eV and a reasonably strong one in the singlet ($2\sigma \rightarrow 2\pi$) transition at about same energy region. Quantitatively, it is seen that our DW ICSs for the transitions leading to the triplet excited states are very similar in the entire energy range. This fact is somewhat expected, since the calculated DCSs for these transitions are similar. Nevertheless, it is interesting to see that the ICSs calculated for the transitions leading to the singlet excited states also become similar at the high end of incident energies. It is worth pointing out that the calculated ICSs for the ($2\sigma \rightarrow 2\pi$) singlet and triplet transitions in CO are significantly larger than their counterparts in C_2H_2. In our previous study, it was shown [8,9] that the ICSs for the promotion of a C($1s$) electron to the lowest unfilled valence orbital for a series of outer-valence isoelectronic molecules with one carbon atom such as CO_2, OCS, and CS2 are, in general, similar to each other, particularly at high incident energies. Therefore, the significant difference seen in the calculated ICSs for these transitions in CO and C_2H_2 seems to indicate that the nonatomic (multicentric) character of the K-shell $1\sigma_{g,u}$ orbitals in acetylene, in contrast to the atomic character of the 2σ orbital of CO (centered mainly on one nucleus), may have some influence in the electron-impact excitation dynamics, even though the energies of those molecular orbitals are very similar to that of the $1s$ orbital of carbon atoms, and the chemical bond energies are negligibly small. Indeed, the remarkable similarity between the ICSs for the ($1\sigma_{g,u} \rightarrow 1\pi_g$) transitions in C_2H_2 at the high end of incident energies, even though the $1\sigma_g$ is bonding and the $1\sigma_u$ is antibonding, seems to confirm that the multicentric character of both orbitals plays as important role for core-excitation processes in C_2H_2.

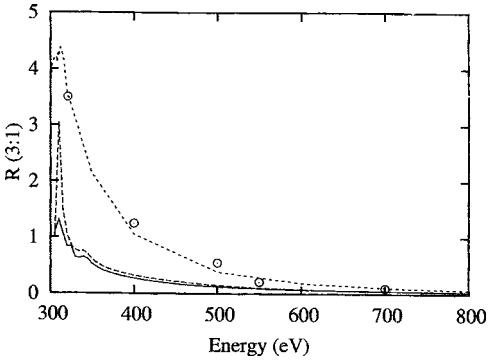

FIG. 7. Calculated triplet-to-singlet ratios RI(3:1). Solid line, for $1\sigma_g \rightarrow 1\pi_g$; dashed line, for $1\sigma_u \rightarrow 1\pi_g$, in C_2H_2; and dotted line, for $2\sigma \rightarrow 2\pi$ transition in CO [7]; open circles, experimental ratio of Almeida *et al.* [20] also for CO.

Figure 7 shows the calculated triplet-to-singlet ratios RI(3:1) obtained by the division of the ICS of the triplet ($1\sigma_g \rightarrow 1\pi_g$) and ($1\sigma_u \rightarrow 1\pi_g$) excitations in C_2H_2, respectively, by the corresponding ICS for the singlet transitions. The calculated [7] and experimental [20] RI(3:1) values for the singlet and triplet ($2\sigma \rightarrow 2\pi$) transitions in CO are also shown for comparison. A sharp peak, located near 309–310 eV and small bumps located at about 325–343 eV are seen in our calculated RI(3:1) values for ($1\sigma_u \rightarrow 1\pi_g$) excitation in C_2H_2. Similar structures, although less pronounced, at about the same energy region are also seen in the calculated RI(3:1) values for the ($1\sigma_g \rightarrow 1\pi_g$) transition. These structures reflect the occurrence of resonances in these energy ranges, or, more accurately, they are due to the energy shift of the resonances in the ICSs of singlet and triplet transitions. In contrast, although pronounced resonance structures are also present in the calculated ICSs for both singlet and triplet ($2\sigma \rightarrow 2\pi$) transitions in CO, they are located at about the same energy region and therefore result in only a small bump in the calculated RI(3:1). Quantitatively, our calculated RI(3:1) values for the ($1\sigma_g \rightarrow 1\pi_g$) and ($1\sigma_u \rightarrow 1\pi_g$) excitations in C_2H_2 are also quite similar, particularly at higher incident energies. The calculated and measured ratios for CO are significantly larger.

In summary, the present work reports an application of the DWA for studying the singlet and triplet ($1\sigma_{g,u} \rightarrow 1\pi_g$) core-level excitations in C_2H_2 by electron impact in the 300–800 eV energy range. Unlike what was observed in our previous studies [8,9] where the excitation ICSs for promotion of a C($1s$) electron to the first unfilled valence orbital in CO_2, OCS, and CS_2 are similar, the presently calculated ICSs for acetylene are in general much smaller than those calculated for CO [7], even at incident energies as high as 800 eV. The calculated ratios RI(3:1) also follow the same trend of the ICSs. Moreover, it is observed that the calculated ICSs for the triplet ($1\sigma_{g,u} \rightarrow 1\pi_g$) transitions are very similar to each other, and this also happens for the singlet transitions at higher energies. Since the binding energies of the $1\sigma_{g,u}$ orbitals in acetylene and the C($1s$) orbital are similar, we suspect that the multicentric character of the core orbitals of C_2H_2 (due to the presence of two carbon atoms), in contrast

to the monocentric character of the 2σ orbital in CO, is responsible for the difference seen in the calculated core-excitation ICSs of the two molecules. Certainly, further investigations on core-excitation processes for more targets with two or more carbon atoms would help to clarify this point. Efforts in this direction are under way.

ACKNOWLEDGMENTS

This research was partially supported by the Brazilian Agencies CNPq, FUNPAR, Fundação Araucária, and FAPESP. Two of us (E.V. and H.L.O.) thank CNPq for partial financial support.

[1] A. P. Hitchcock, J. Electron Spectrosc. Relat. Phenom. **112**, 9 (2000).
[2] G. C. King, M. Tronc, F. H. Read, and R. C. Bradford, J. Phys. B **10**, 2479 (1977).
[3] I. Harrison and G. C. King, J. Phys. B **19**, L447 (1986).
[4] I. Harrison and G. C. King, J. Electron Spectrosc. Relat. Phenom. **43**, 155 (1987).
[5] C. E. Blount and D. M. Dickinson, J. Electron Spectrosc. Relat. Phenom. **61**, 367 (1993).
[6] T. Kroin, S. E. Michelin, K. T. Mazon, D. P. Almeida, and M.-T. Lee, J. Mol. Struct.: THEOCHEM **464**, 49 (1999).
[7] T. Kroin, S. E. Michelin, and M.-T. Lee, J. Phys. B **34**, 1829 (2001).
[8] S. E. Michelin, T. Kroin, A. S. Falck, E. A. y Castro, O. Pessoa, H. L. Oliveira, and M.-T. Lee, J. Phys. B **36**, 1525 (2003).
[9] T. Kroin, S. E. Michelin, A. S. Falck, F. Arretche, I. Iga, and M.-T. Lee, Phys. Rev. A **68**, 012701 (2003).
[10] M. P. Miranda, C. E. Bielschowsky, H. M. Boechat-Roberty, and G. G. B. de Souza, Phys. Rev. A **49**, 2399 (1994).
[11] A. P. Hitchcock, A. P. Johnston, T. Tyliszczak, C. C. Turci, M. M. Barbatti, A. B. Rocha, and C. E. Bielschowsky, J. Electron Spectrosc. Relat. Phenom. **123**, 303 (2002).
[12] A. W. Fliflet and V. McKoy, Phys. Rev. A **21**, 1863 (1980).
[13] L. M. Tao and V. McKoy, J. Phys. B **15**, 3971 (1982).
[14] M.-T. Lee, L. M. Brescansin, and M. A. P. Lima, J. Phys. B **23**, 3859 (1990).
[15] M.-T. Lee, S. E. Michelin, T. Kroin, L. E. Machado, and L. M. Brescansin, J. Phys. B **28**, 1859 (1995).
[16] R. R. Lucchese, G. Raseev, and V. McKoy, Phys. Rev. A **25**, 2572 (1982).
[17] U. Fano and D. Dill, Phys. Rev. A **6**, 185 (1972).
[18] T. H. Dunning, J. Chem. Phys. **55**, 716 (1971).
[19] W. J. Hunt and W. J. Goddard, Chem. Phys. Lett. **24**, 464 (1974).
[20] D. P. Almeida, G. Dawber, G. C. King, and B. Palasthy, J. Phys. B **32**, 3157 (1999).